Solar Energy Materials & Solar Cells 253 (2023) 112245

Contents lists available at ScienceDirect

Solar Energy Materials and Solar Cells

journal homepage: www.elsevier.com/locate/solmat

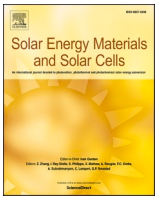

Assessing the stability of p^+ and n^+ polysilicon passivating contacts with various capping layers on p-type wafers

Chukwuka Madumelu [a,*], Yalun Cai [a], Christina Hollemann [b], Robby Peibst [b,c], Bram Hoex [a], Brett J. Hallam [a,d], Anastasia H. Soeriyadi [a,e]

[a] School of Photovoltaic and Renewable Energy Engineering (SPREE), UNSW, Sydney, NSW, 2052, Australia
[b] Institute for Solar Energy Research Hamelin (ISFH), Am Ohrberg 1, 31860, Emmerthal, Germany
[c] Institute of Electronic Materials and Devices, Leibniz Universität Hannover, Schneiderberg 32, 30167, Hannover, Germany
[d] ITP Renewables, Level 10, Christie Spaces, 3 Spring St. Sydney NSW, Australia
[e] Department of Materials, University of Oxford, Oxford, United Kingdom

A B S T R A C T

Polysilicon (poly-Si)-on-oxide passivating contact structures (POLO/TOPCon) enable high-efficiency solar cells as they simultaneously provide a very high level of surface passivation and a high conductance for either electrons or holes. The ease of incorporation with existing manufacturing lines and their tolerance for high-temperature processing has increased the wide acceptance of this structure in the PV industry. In this report, we explore the effects of short high-temperature annealing required for effective hydrogenation and formation of ohmic screen-printed contacts across a wide temperature range (636 °C–846 °C) on the stability of passivating contact structures. We study this on p-type c-Si substrates with phosphorus-doped (n-type) or boron-doped (p-type) polysilicon contacts capped with either an AlO_x or SiN_x coating. Our experimental results show that irrespective of the poly-Si doping type, AlO_x-capped samples suffer a loss in surface passivation across the investigated temperature range, while SiN_x-capped samples show an improvement at lower annealing temperatures. Above 744 °C, severely ruptured blisters occur for the samples coated with a SiN_x layer, leading to lift-off of the poly layer in extreme cases, and in all cases, significant surface passivation losses, up to 99%. A study of the long-term stability of these fired samples under 1-sun illumination @ 140 °C shows that they suffer from both bulk and surface-like instabilities. Two degradation cycles were observed: the first, a boron-oxygen light-induced degradation (BO-LID) observed after 5 min, with capture cross-section ratios of 15.8–19.2, and a slower secondary degradation, similar to light and elevated temperature-induced degradation (LeTID), with maximum degradation reached after ~ 14 days. The presence of a silicon nitride layer does not appear to influence the kinetics of post-degradation recovery. Our results suggest that the effect of firing may be influenced by the polarity of the bulk c-Si or perhaps the chemistry of the SiN_x film and highlight that passivating contact structures based on p-type c-Si may offer better long-term stability than those based on n-type c-Si.

1. Introduction

The solar cell market is currently dominated by silicon solar cells, specifically, the passivated emitter and rear cell (PERC) architecture [1]. Efficiency limits imposed by high recombination losses in the phosphorus-doped emitter of the PERC cell have prompted researchers to develop alternatives. One of the most promising solutions is using passivating contacts based on SiO_2/polysilicon (SiO_2/poly-Si), in which the most popular approach, currently, is a cell architecture based on an n-type substrate with a boron emitter on the front with a rear SiO_x/-poly-Si stack. Remarkable surface passivation and extremely low recombination current density parameter, J_0, less than 5 fA/cm [2,3,], have been shown, with demonstrated record efficiency of 26.1% on an industrial n-type wafer design. While on p-type Si, Haase et al. utilized a rear contact geometry to achieve a record efficiency of 26.1% [4], and Richter et al. demonstrated a both-sides-contacted cell with 26% efficiency [5].

However, recent studies have raised concerns about the stability of passivating contact structures, highlighting potential surface and bulk instabilities resulting from the high-temperature firing step required for metallization. Winter et al. observed bulk-related BO defects in p-type Si and surface degradation and recovery on both n- and p-type Si after light soaking fired samples with n-poly contacts. It was observed that the changes in surface passivation also occurred during dark annealing, with J_0 increasing up to a factor of five after light soaking [6]. Kang et al. also showed that similar surface-related degradation and recovery occurred in n-type Si with poly contacts, deposited either via plasma-enhanced chemical vapor deposition (PECVD) or low-pressure chemical vapor deposition (LPCVD). In that study, it was also observed that the rate of surface degradation was influenced by the temperature during light

* Corresponding author. School of Photovoltaics and Renewable Energy Engineering, University of New South Wales, Kensington 2033, Sydney, Australia.
E-mail address: c.madumelu@unsw.edu.au (C. Madumelu).

https://doi.org/10.1016/j.solmat.2023.112245
Received 15 November 2022; Received in revised form 18 January 2023; Accepted 14 February 2023
Available online 19 February 2023

soaking (LS) and that the silicon nitride layer after firing was required for recovery of surface passivation [7]. Chen et al. showed that in n-type Si, a higher LS temperature accelerated the degradation and recovery kinetics and reduced the extent of degradation and suggested that a complete degradation and recovery cycle was sufficient to mitigate the responsible defect [8].

Although the high-efficiency potential of p-type poly has been demonstrated in the lab with a 26.1% efficient POLO-IBC structure [9], the firing and long-term stability of p-poly structures have not been extensively studied. On p-type Si with poly contacts, Hollemann et al. observed a J_0 increase after firing above 600 °C and highlighted that the changes in J_0 were influenced by the speed of the belt furnace [10]. Also, in a previous communication, we showed the injection-dependent lifetime spectroscopy (IDLS) results of both AlO_x and SiN_x-capped n- and p-poly samples, tested under accelerated conditions [11]. In that work, we observed a degradation during LS and dark annealing (DA) under accelerated testing conditions for AlO_x and SiN_x-capped samples. For AlO_x capped samples, while p-poly Si samples were stable under the testing conditions, n-poly degraded at a similar rate during LS and DA, with no observable recovery in lifetimes occurring during the testing period. For SiN_x-coated samples, the degradation was positively correlated with firing temperature, with higher firing temperatures showing more degradation and complete recovery after 100 s. Such accelerated conditions allow testing to be carried out in timescales in seconds by accelerating the degradation/recovery kinetics [12–15]. Different reasons have been suggested for the instabilities observed, including an excess of hydrogen in the interface layers [16] and increased thermal stress during the firing process or a combination of them [10].

In this paper, as an extension to previous work [11,17], we investigate the effect of high-temperature firing on p-type Si symmetrically coated with n- and p-poly layers. Further, we examine their long-term stability during 1-sun illuminated annealing conditions. We apply Fourier transform infrared (FTIR) spectroscopy and time-of-flight secondary ion mass spectroscopy (ToF-SIMS) to analyze the hydrogen content in the cell precursors and correlated them to the observed changes in passivation. Specifically, we show that the firing of p-type Si with poly contacts will improve surface passivation under certain conditions. We also show that above a certain temperature threshold, firing is detrimental and can lead to blistering of the poly layer and significant surface degradation. Subsequently, we show that light soaking can lead to bulk and surface instabilities, however, they are significantly less severe than observed in n-type Si. This may imply that p-type Si with passivating contacts may be intrinsically more stable than their n-type counterparts.

2. Methodology

The test structures studied in this work consisted of p-type (boron-doped) Czochralski, 20 Ω-cm Si wafers. All samples were etched in KOH solution to remove saw damage which produced a planar surface and subsequently cleaned using the Radio Company of America (RCA) methodology. A 1.5 ± 0.2 nm thick silicon oxide layer was grown on both sides by a wet chemical process using ozone. The oxide was capped with a 200 nm-thick poly-Si deposited using a CENTROTHERM EUROPE 2000 low-pressure chemical vapor deposition (LPCVD) with *in-situ* n- or p-type doping using gas precursors PH_3 and BCL_3 respectively. After the poly Si deposition, the samples were annealed for 30 min in a Tempress TS81004 tube furnace at 820 °C. Following this, the surface silicon oxide grown on the poly-Si surface was etched using a 40% HF solution, leading to a poly-Si thickness of about 140 nm. For each doping type (n^+ or p^+), the samples were split into two groups: one group was symmetrically coated with a 100 nm thick SiN_x layer with a refractive index of 2.05 at 600 nm deposited using an inductively coupled plasma chemical vapor deposition (IC-PECVD) Singular XP tool. For the other split, the sample was symmetrically coated with a 10 nm atomic layer deposition (ALD) AlO_x layer using an Ultrafast ALD tool by SoLayTEC and subsequently annealed at 425 °C for 30 min in an N_2 atmosphere.

All samples were subsequently fired in an industrial belt-firing furnace (SCHMID/Sierratherm Thermal Furnace System), using a typical temperature profile for the firing of metallization pastes, at a peak (measured) temperature range between 646 °C and 836 °C, and a belt speed of 5.6 m/min. Some samples subsequently had a dielectric etch in HF and followed by a rapid thermal anneal (RTP) in an N_2 atmosphere at 300 °C.

For the stability studies, the fired samples were split into two: one group with a SiN_x capping layer and the other group with the SiN_x layer etched in dilute HF. Both groups were annealed at 140 °C on a hot plate under ~1-sun illumination from four halogen lamps. The hot plate temperature was verified with a digital multi-meter with K-type thermocouples, and the illumination intensity was calibrated to 1 kWm^{-2} using a ThorLabs PM100D power meter. The electronic quality of the structures was evaluated by quasi-steady-state photoconductance decay (QSSPC) measurements using a Sinton WCT-120 lifetime tester. The effective minority carrier lifetime, τ_{eff} was extracted at $\Delta n = 2 \times 15/cm^{3,}$ and J_0 was extracted using the Kane and Swanson method [18]. Time-of-flight secondary ion mass spectrometer (ToF-SIMS) profiling was done using an ION-TOF TOF-SIMS 5 spectrometer, and Fourier transform infrared spectroscopy (FTIR) was carried out on a PerkinElmer Spectrum Two FTIR tool. Raman analysis was carried out on a Reinshaw InVia 2 Raman tool.

3. Results and discussion

3.1. Impact of firing temperature on n- and p-type poly-Si with various capping layers

First, we investigate the effects of an industrial belt-furnace firing step on the performance of samples with phosphorus-doped and boron-doped poly-Si/SiO_x layers. For each case, firing at a peak temperature, T_F, between 646 °C and 836 °C was carried out on samples with either an AlO_x or SiN_x capping layer.

3.2. AlO_X capping layer

Fig. 1 shows the τ_{eff}, J_0, and iV_{OC} for p- and n-poly, AlO_x-coated samples before and after firing, for a range of T_F (675 °C and 836 °C). Before firing, the p-poly and n-poly samples have quite different τ_{eff} and J_0 values. Most p-poly samples had τ_{eff} values around the 1 ms mark and J_0 values above 70 fA/cm^2. The n-poly samples had τ_{eff} values greater than 3 ms and J_0 values lower than 20 fA/cm^2. Within each category, the differences in τ_{eff} resulted from spatial non-uniformity across wafers, most likely resulting from experimental non-uniformities in poly-Si deposition or dielectric deposition.

For both p- and n-poly samples, firing resulted in an increase in J_0 and a decrease in $\tau_{eff,}$ for all investigated peak firing temperatures. For the p-poly samples, firing above 725 °C led to a noticeable increase in $J_{0,}$ which was even more significant after firing at 836 °C. Overall, the firing temperature did not have a strong correlation with J_0, with an average J_0 increase of 32 fA/cm^2 observed for all investigated firing temperatures. This remarkable stability in surface passivation provided by the p-poly AlO_x-capped layers is also evidenced in the modest decrease in $iV_{OC,}$ with an average loss of ~9 mV across all firing temperatures.

For the n-poly samples, the reduction in τ_{eff} increased with increasing peak firing temperature. On average, τ_{eff} decreased by ~20% across all firing temperatures for T_F between 675 °C and 725 °C, with a greater decrease for $T_F > 725$ °C and even up to 60% loss after firing at 836 °C. The changes in τ_{eff} were related to a reduction in surface passivation, with a notable increase in J_0 with increasing firing temperature. A maximum increase of more than 400% was observed for the samples fired at 836 °C. Such severe surface degradation observed in n-poly samples at high temperatures can significantly impact device performance, as seen in the changes in $iV_{OC,}$ with losses of up to 35 mV. On the

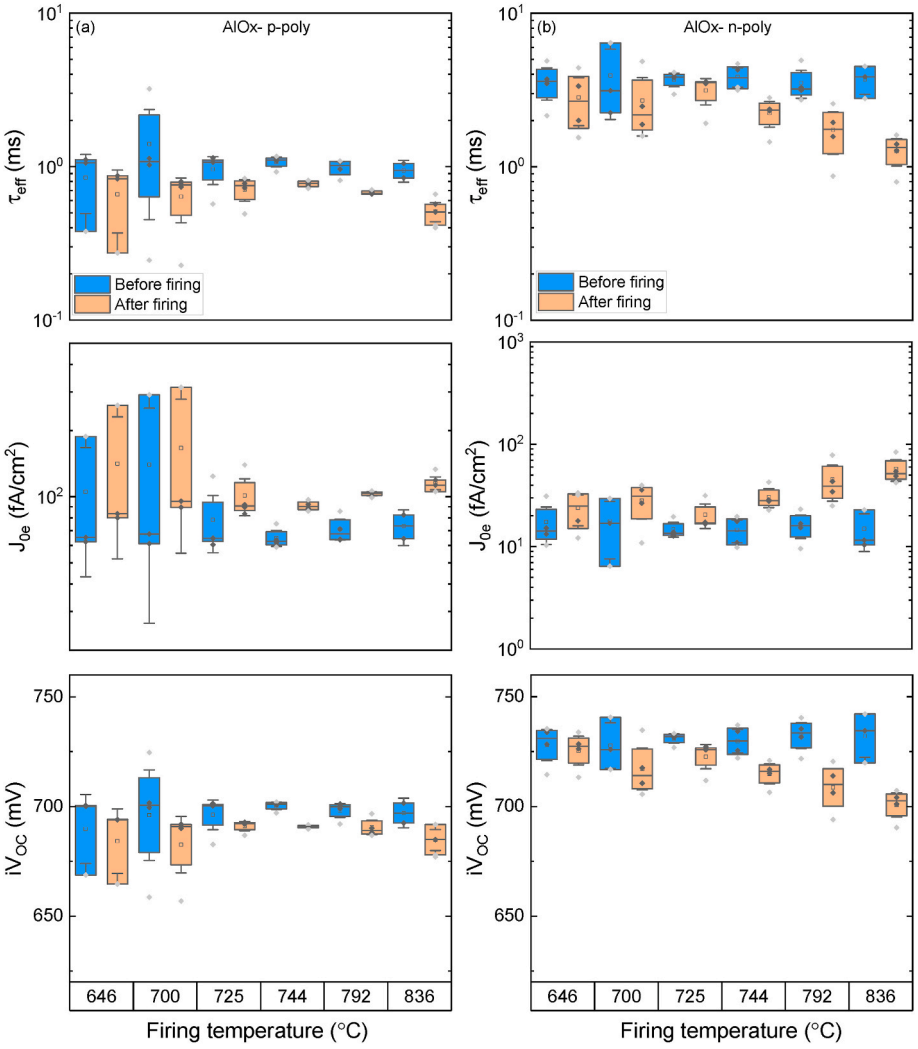

Fig. 1. τ_{eff} (extracted at $\Delta n = 2 \times 15/cm^3$), J_0 and iV_{OC} before and after belt furnace firing at various temperatures for symmetrical **AlO_x**-capped (a) p-poly samples, and (b) n-poly samples.

other hand, firing at a lower temperature of 675 °C caused a slight decrease of ~2 mV. From Fig. 1, we observe the superior firing stability of p-poly samples over their n-poly counterparts, which reduces the comparative advantage of n-poly samples after a high-temperature firing step, as illustrated by closer iV_{OC} values to p-poly samples after firing.

3.3. SiN_X capping layer

In Fig. 2, the τ_{eff}, J_0, and iV_{OC} for double-sided SiN_x-capped p- and n-poly samples, before and after firing are presented. Like for the AlO_x-capped samples, the starting τ_{eff} is greater for n-poly samples, illustrating their superior passivation compared to p-poly samples. Except for $T_F \geq 792$ °C, firing improved the level of surface passivation of both p- and n-poly samples, as evidenced by the higher (lower) values of τ_{eff} (J_0) after firing. In p-poly, the average minimum improvement in τ_{eff} (+120%), J_0 (- 58%), and iV_{OC} (3%) occur after firing at the lowest temperature of 675 °C. Increasing T_F led to even more significant improvements, although a higher temperature gradient at higher temperatures may have caused increased sample-to-sample variability.

Likewise, for the n-poly samples, enhancements in passivation quality were also observed after firing. However, the improvements after firing do not correlate with T_F. Interestingly, although the starting iV_{OC} values were higher in n^+ poly than in p^+ poly samples, the improvements after firing were at par, with even less variability among the p-poly samples. These observations are in stark contradiction to our previous work [8], where we showed that firing at similar T_F ranges as used in this work was detrimental to n-poly passivation on n-type c-Si. Kang et al. also reported that firing at 700 °C led to a deterioration of surface passivation for both p-and n-poly on n-Si, with greater stability observed in p-poly samples [19]. The major difference between this study and those was the polarity of the Si bulk (p-type in this study versus n-type in the others). It is thus possible that the stability of the surface passivation after firing is dependent on the polarity of the bulk material and requires further investigation.

For both polysilicon doping categories (p- and n-poly), firing at $T_F \geq$ 792 °C was detrimental and caused a severe loss in surface passivation. The effect of firing-induced damage was more evident in p-poly samples fired at 836 °C, with over 97% loss in τ_{eff} and J_0 increasing by over two orders of magnitude (>1000 fA/cm^2) and a significant reduction in iV_{OC} (up to 132 mV). For the n-poly samples, the deterioration, although significant, was to a lesser extent than for the p-poly samples. For $T_F \geq$ 792 °C, blistering of the SiN_x/poly layers was seen in both p- and n-poly samples and is likely responsible for the disparate firing response at these higher temperatures. Fig. 3 shows micrographs taken with an optical microscope and a scanning electron microscope (SEM) of p-poly samples. Some of the samples (Fig. 3 a-d) have a SiN_x-capping layer, while some (Fig. 3 e-f) had the nitride layer removed in dilute HF

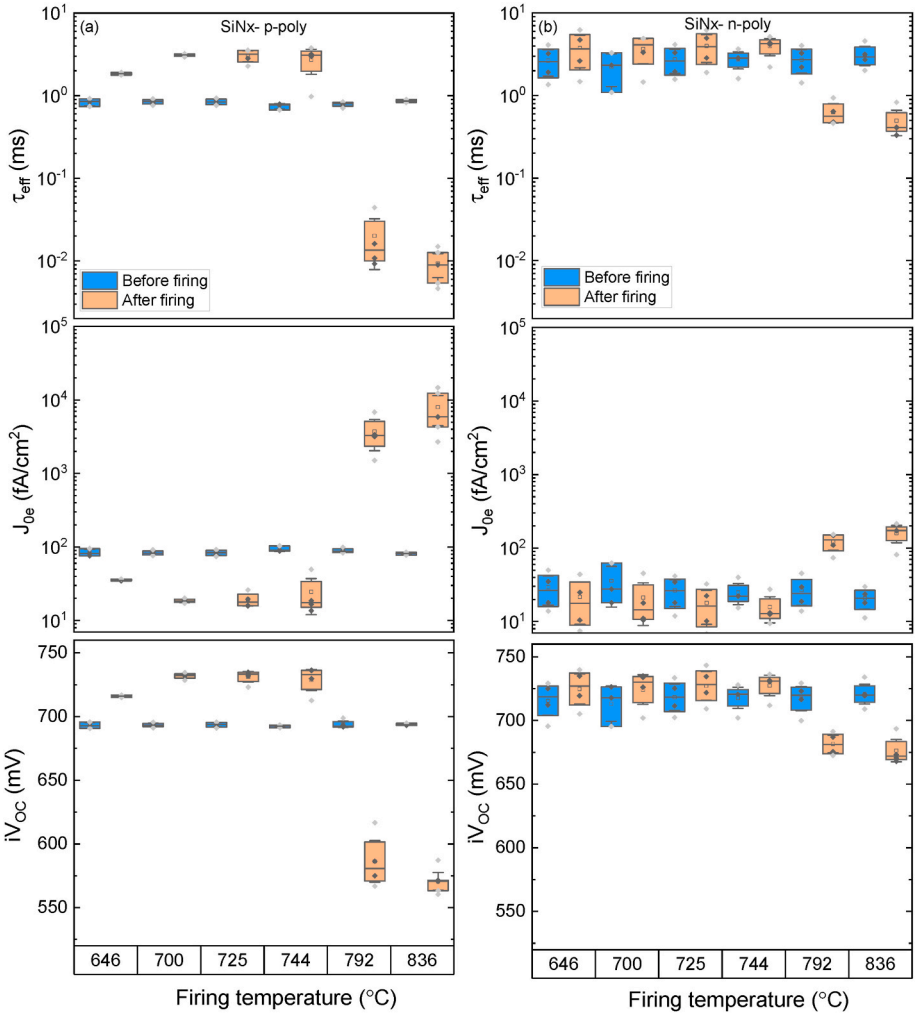

Fig. 2. τ_{eff} (extracted at $\Delta n = 2 \times 15/cm^3$), J_0 and iV_{OC} before and after belt furnace firing at various temperatures for symmetrical **SiN$_x$**-capped (a) p-poly samples, and (b) n-poly samples.

solution. Fig. 3a and b shows images taken from an optical microscope and SEM, respectively, before firing. After firing at 836 °C, ruptured blisters of the SiN_x film can be seen (white patches, Fig. 3c), which were not seen before firing (Fig. 3a). Cross-sectional SEM imaging (Fig. 3d) reveals delamination of the SiN_x/poly layers in some of the samples on which blistering is observed, indicating a physical removal of the passivating contacts on those samples. The blistering is likely caused by an infusion of excess hydrogen, released from the SiN_x layers during firing. Blister formation is suggested to be due to an accumulation of hydrogen at the poly/SiO_x/c-Si interface, with more significant blistering observed in PECVD-deposited a-Si films, due to the hydrogen-rich precursor gases and the deposition conditions employed [20,21]. Such excess hydrogen may build up in the poly-Si interface and eventually lead to delamination of the poly layer [20–22], leading to a significant loss of surface passivation as seen in Fig. 2. To further investigate the role of SiN_x in the formation of blisters, some p-poly samples with SiN_x capping layers were dipped in HF solution to strip off the hydrogen-rich SiN_x films before firing at 836 °C. The samples were completely hydrophobic to ensure the complete removal of the SiN_x films before firing. Fig. 3e and f shows the micrographs of the samples after the HF dip and firing, respectively. The ruptured blisters seen in SiN_x -capped samples (Fig. 3c) after firing were not visible in samples in which the nitride layers were stripped prior to firing and provide strong evidence to suggest that the presence of the SiN_x layer during firing is a prerequisite for the blistering to occur. Besides providing a rich source of hydrogen during firing, the layer will also act as an effusion barrier to prevent the escape of already released hydrogen. We note, however, that, unlike SiN_x-capped samples in which the lifetimes improve after firing at $T_F <$ 792 °C, the firing of the uncapped samples at 836 °C still led to a loss in surface passivation. This result implies that blistering and delamination of the SiN_x/poly layers is likely not the only factor contributing to the deterioration in surface passivation after firing at higher temperatures, which was shown before [17,23], but requires further investigation to clarify the cause. Noteworthy is the fact that the measured τ_{eff} (J_0) after firing was one order of magnitude higher (lower) compared to the samples which were capped with the SiN_x layer during firing.

In finished cells, ruptured blisters can form a pathway for metal diffusion into the material and potentially allow metals to come in direct contact with Si during firing and exacerbate device degradation [21]. There have been suggestions that blistering and lamination are more severe in samples with chemically-grown tunneling oxide layers due to their off-stoichiometry and lower density [21]. However, this assertion disagrees with recent work by Firat et al. where more blistering occurred in devices that featured thermally-grown tunneling oxides [22].

Fig. 4a displays the Raman spectra of n- (red) and p- (blue) poly films before (dashed lines) and after firing (solid lines) at $T_F = 836$ °C. As a reference, the Raman spectrum of a-Si on a glass slide (transparent in Raman spectroscopy), scaled to have a similar peak area to those of the poly samples, is also shown (green). The clear difference in the peak position of the reference a-Si (475 cm^{-1}) vs poly-Si (515-520 cm^{-1}) and

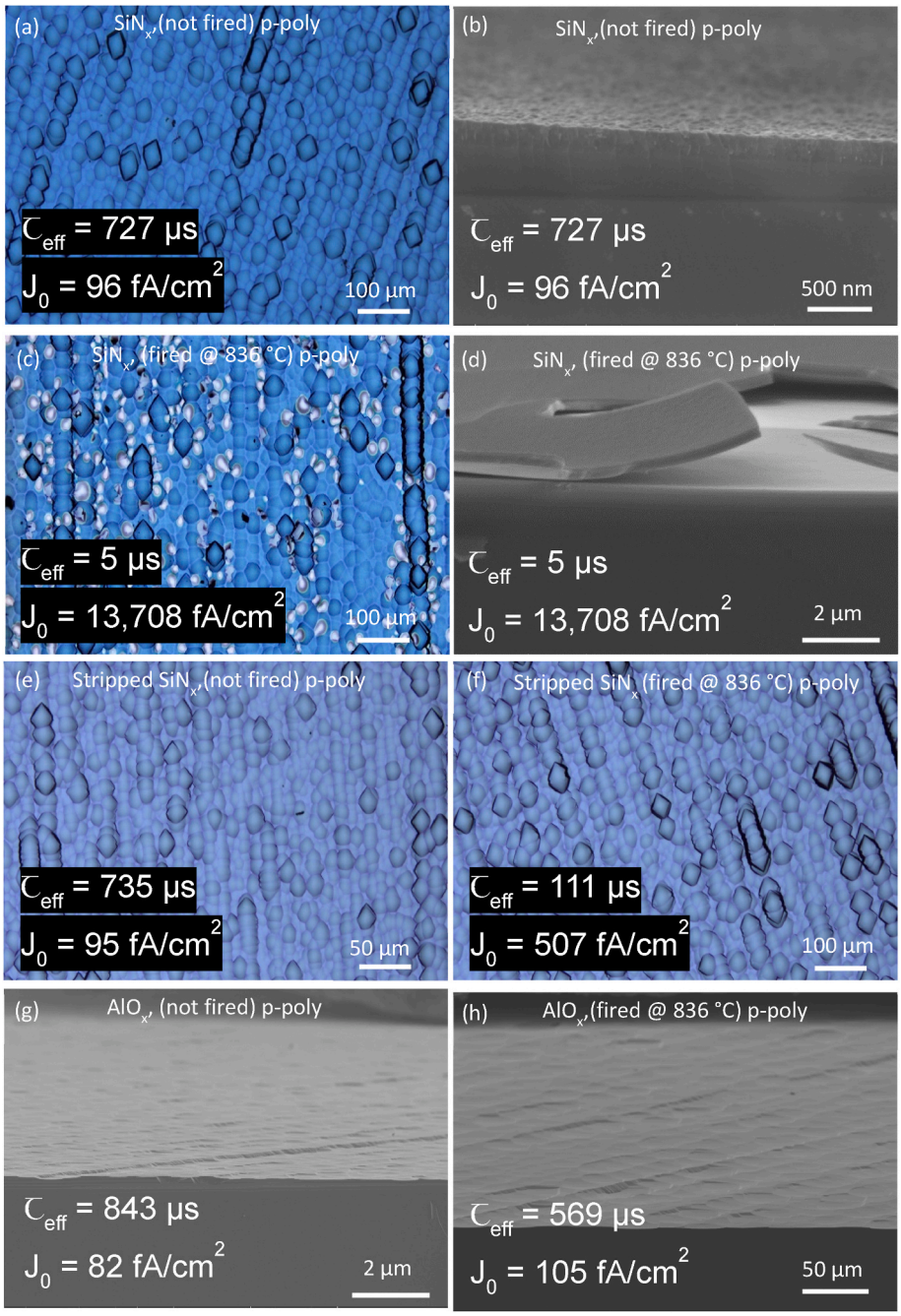

Fig. 3. Micrographs obtained from an optical microscope (OP) and cross-sectional scanning electron microscope (SEM), for SiN_x-capped p-poly samples (a) before firing-OP (b) before firing- SEM (c) after firing at 836 °C–OP (d) after firing at 836 °C -SEM (e) after a SiN_x etch in HF only- OP (f) after a SiN_x etch in HF and then fired at 836 °C- SEM (g) AlO_x-capped p-poly sample before firing- SEM (h) AlO_x-capped p-poly sample after firing at 836 °C - SEM.

c-Si (520 cm^{-1}) suggests that the poly layers were not in their hydrogen-rich a-Si state, but almost fully crystallized before firing. Therefore, the blistering during the firing process was likely caused by hydrogen from the SiN_x capping layer. The reduction in the full width half maximum (FWHM) of the characteristic c-Si peak during the firing process can be explained by the relaxation of stress in the microstructure of the poly-Si layer, agreeing with the expectation that firing may contribute to further crystallinity, as observed on the p-poly sample. As a result, the non-crystallinity of the poly-Si layer can be ruled out when considering the cause(s) of lifetime degradation after firing. Fig. 4b shows a clear trend of decreasing *N*–H stretching absorption band peak area extracted from Fourier transform infrared (FTIR) measurements after firing at different temperatures. The lower *N*–H bond density after firing suggests a higher release of hydrogen from the SiN_x layers at higher temperatures, potentially leading to a higher accumulation at the poly/SiO_x/c-Si interfaces. However, we should state that the samples used in this work featured planar surfaces, which have been suggested to have more significant blistering and delamination than textured surfaces due to a lower film adhesion force [20,24]. Notwithstanding, the work by Firat et al. carried out on textured surfaces also exhibited blistering. The importance of the blistering and delamination effects requires more attention, especially given that the temperature range in which this is typically observed coincides with the high-temperature firing sequence needed for the metallization of solar cells.

The lower hydrogen content in LPCVD Si films, higher deposition temperatures employed and the already high crystallinity (Fig. 4a) of the

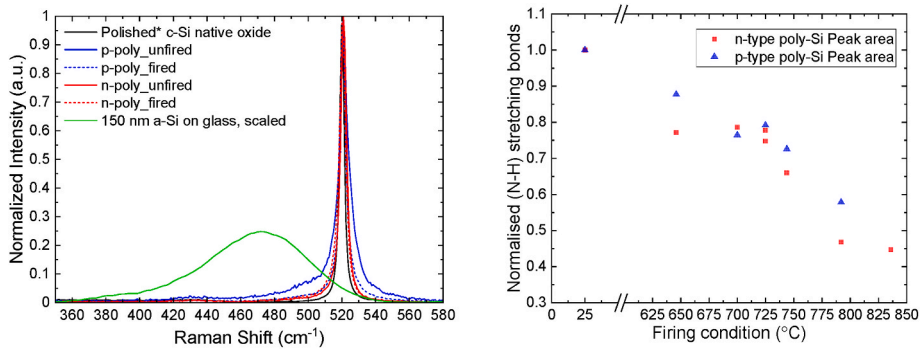

Fig. 4. (a) Raman spectra of unfired and fired (T_F = 836 °C) poly samples, shown with as-deposited a-Si for reference (b) Normalised FTIR data showing *N*–H stretching bonds in n-and p-poly samples.

passivating contact layers before firing make the formation of blisters in this work, unexpected. Notably, our work shows that at $T_F \geq 792$ °C, B-doped poly samples exhibit higher blistering (and post-firing degradation) than *P*-doped poly samples. This again is in contradiction to enhanced post-firing stability observed in p-poly samples in other works [19,25]. A notable difference in the structure used in this work and those in other works, including from the authors of this work, is the base doping polarity of the c-Si wafer. In other works, firing-induced degradation occurs when SiN_x is used as a capping layer (irrespective of the poly doping) in n-type c-Si, a significant improvement is observed herein in p-type c-Si. Thus, suggesting that the firing response in poly contacts is dependent on the doping polarity of the Si bulk. This may be related to the different charge states of hydrogen in the c-Si bulk, which depends on the Fermi level, and the resulting diffusion coefficient, particularly during the heating and cooling steps. There is also the possibility that the specific deposition tool employed (IC-PECVD) or the composition of the nitride film may play some role in the observed behaviour. In Fig. 5, the percentage change in J_0 after firing polysilicon contacts with capped SiN_x films is shown, extracted from other works in the literature. The symbols in red are for n-type wafers, while those in blue are for p-type. For most of the studies examined, various processing parameters such as base doping, SiN_x film deposition parameters, and firing belt speed were varied. We observe that most of the J_0 increase after firing occurs in n-type c-Si samples. A notable exception is the work by Morisset et al. on n-type c-Si where reductions in J_0 after firing were observed for samples

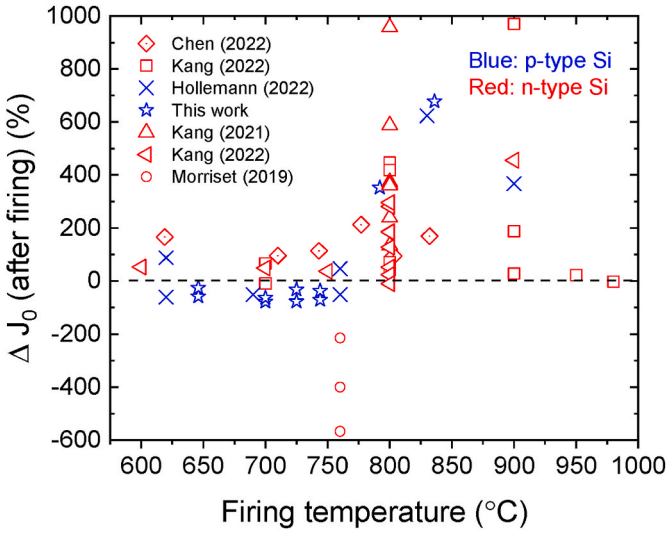

Fig. 5. Percentage changes in J_0 after firing as a function of firing temperature compiled from literature [8,17,53–55]. Blue symbols are for p-type c-Si, and red for n-type c-Si.

on which deposition parameters were optimized for a lower hydrogen content[55]. On the other hand, on most p-type c-Si substrates, there was a net reduction in J_0 after firing. We note, however, that there are limited studies on passivating contacts on p-type c-Si. Nonetheless, our results indicate that the base doping polarity or perhaps the composition of SiN_x or deposition tool employed, may influence changes in the surface passivation response to firing.

Regarding field-effect passivation, dielectric films such as AlO_x and SiN_x deposited on silicon provide fixed charges which can modify the surface state of materials, with the former exhibiting negative fixed charges and the latter positive charges [26,27]. However, the Debye length in the grown poly-Si sample is usually much smaller than the thickness employed in making passivating contacts. Thus, the influence of the fixed charges by dielectrics is screened by the highly doped poly layer, with exceptions in very thin poly-Si with low doping. In a separate firing study (not shown), the authors did not observe any significant difference in the diffused dopant concentration after firing. Hence, firing was not expected to influence the concentration of electrically active dopants within the poly-Si layer/c-Si substrate. The AlO_x samples employed in this study were annealed at 425 °C for 30 min in N_2, before the firing results are shown in Fig. 1.

3.4. Dehydrogenation after HT firing

As observed in the previous sections, the passivation quality of fired samples is strongly related to the release of hydrogen and its complicated interaction with different layers of the structures. Indeed, while the positive effects of hydrogenation in improving the performance of solar cells are widely acknowledged [28,29], hydrogen has also been shown to be responsible for the formation of recombination centres [30], dopant deactivation [30], formation of structural defects [31] and the creation of vacancy-hydrogen complexes [32], leading to severe bulk and surface lifetime degradation [33,34].

To further understand the role of hydrogen, samples fired at 846 °C were further annealed in N_2 at 300 °C. It has been previously reported that short dehydrogenation in N_2 after a high-temperature firing could be beneficial, since an excess of hydrogen released during firing may be responsible for loss in surface passivation. Kang et al. demonstrated that a short dehydrogenation anneal was sufficient to reverse degradation observed after firing [19]. Two groups were presented: one with the capping layers (AlO_x and SiN_x) present and the other with the capping layers etched off in HF, prior to annealing. The changes in J_0 after annealing in N_2 are depicted in Fig. 6, and for reference, the J_0 values before and after firing are also presented. For all groups, annealing in N_2 after HT firing did not lead to improvements in surface passivation. In samples where J_0 reduces or stabilizes with continual annealing, the level of surface passivation was still considerably lower than in the pre-fired state. On the AlO_x (and AlO_x-stripped) samples in Fig. 6 a and b, annealing at 300 °C in N_2 atmosphere did not lead to improvements in

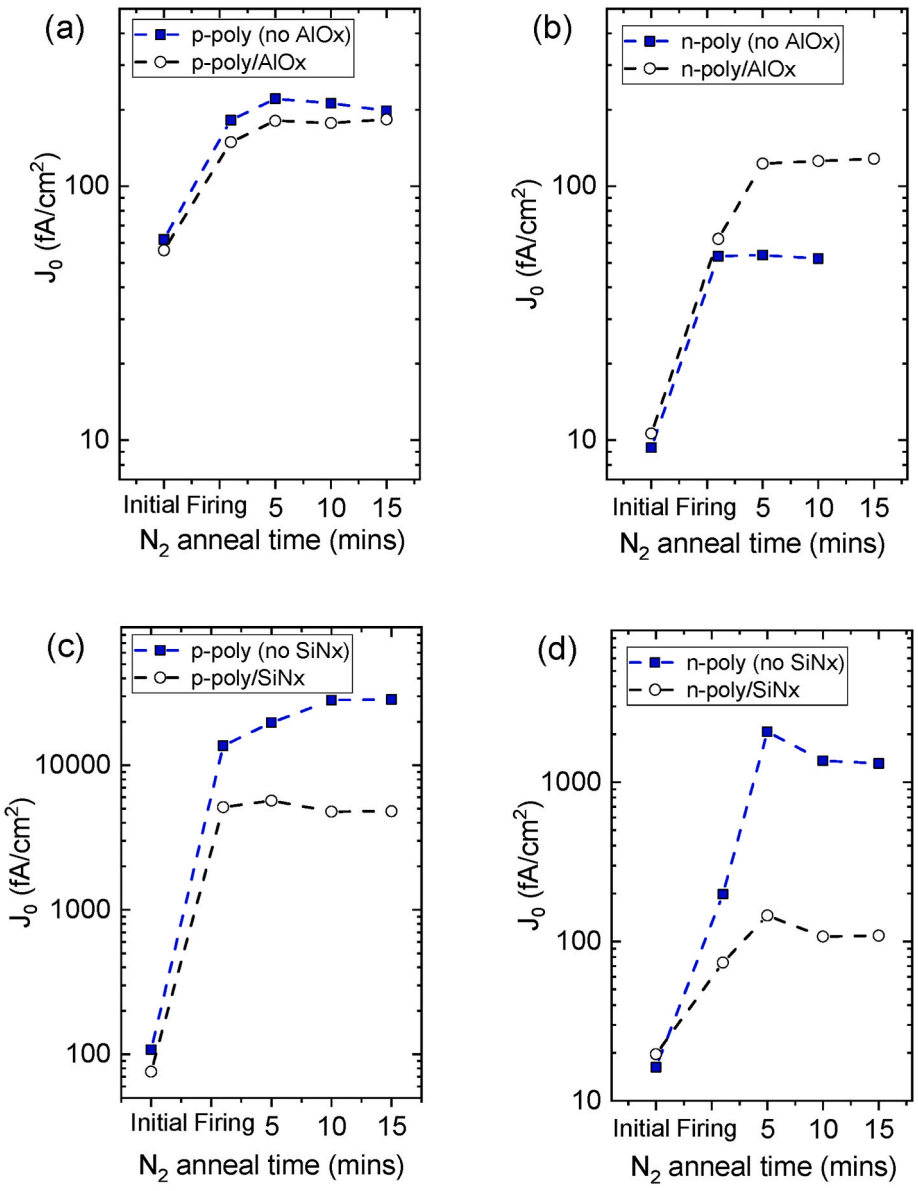

Fig. 6. Changes in J_0 after annealing in N_2 at 300 °C for (a) AlO_x and (b) SiN_x coated samples. The J_0 values before and after firing are indicated for reference.

surface passivation. On the contrary, the J_0 values increased after annealing, except in the n-poly sample without an AlO_x layer, which remained stable during the annealing. The increase in J_0 was greater for the n-poly samples (which had lower initial J_0 values compared to p-poly). The reduction in surface passivation is likely due to a loss in hydrogen after firing, as observed by Van de Loo et al. It was noted that the removal of AlO_x capping layer led to a significant reduction in hydrogen concentration and that samples with an AlO_x capping layer showed much greater stability during annealing in N_2[35]. AlO_x typically contains 2–3% at. % H which provides chemical passivation for defect passivation. However, at about 400 °C, effusion of molecular hydrogen takes place, and the ability of the AlO_x layer to act as a good effusion barrier reduces [36]. Before annealing, the samples had undergone a high-temperature firing process (846 °C) and had already lost a significant amount of hydrogen, which explains the loss in surface passivation after firing. Annealing in N_2 would further dehydrogenate the samples and lead to increased surface deterioration, as observed. The changes in surface passivation, as indicated by the evolution in J_0, may imply that a significant amount of hydrogen was already released into the bulk or effused during the HT firing process and annealing in N_2 was causing a further de-hydrogenation of the samples. For n-poly, the J_0 of the uncapped layer (53 fA/cm^2) was much lower than the capped layer (122 fA/cm^2) after de-hydrogenation, although they had similar J_0 values before the dehydrogenation anneal. Removing the AlO_x layer makes the poly-Si stable during further dehydrogenation. It is possible that with further annealing, the remaining H contained in the AlO_x layer is continually released and builds up at the poly interface since the annealing temperature is not high enough for quick effusion. This explanation does not hold for p-type poly, where the uncapped samples show de-passivation with N_2 annealing. This disparate response to de-hydrogenation in n-poly is not clear and requires further examination.

On the SiN_x samples, annealing without a nitride capping layer was more detrimental to surface passivation for both p- and n-type poly. After 15 min of annealing, samples with a SiN_x capping layer, although with ruptured blisters (Fig. 3c) had considerably lower J_0 (more than 1 order of magnitude) than samples w/o a capping layer. This is in contrast to observations by Kang et al. [23], where it was shown that annealing in N_2 after an 800 °C firing step improved surface passivation. Kang et al. showed that in samples where the SiN_x capping layer had

been removed, annealing for up to 40 min at 300 °C led to improvements in surface passivation because of reduced H concentration around the tunneling oxide layer. Presumably, however, these samples were not blistered, which is not stated in the paper. Without a capping layer, H effusion is expedited, leaving the precursors with much less H for passivation. There is also the effect of reduced light-coupling due to SiN_x removal, which could also negatively impact the device.

It is clear that for both AlO_x and SiN_x-coated samples, the removal of "excess" hydrogen via a dehydrogenation step can further deteriorate surface passivation. Although in the blistered samples, the non-uniformity caused by local removal of the poly contacts in some regions, makes a direct comparison with non-blistered samples difficult. But the results show that a dehydrogenation step is not necessarily a good step and may even lead to further surface degradation.

3.5. Effect of long-term stability testing on p- and n-poly layers

In this section, we explore the effects of long-term stability testing for SiN_x-coated poly samples, under 1-sun illumination conditions at 140 °C, following the fast-firing step.

Herein, we examine n-and p-poly structures, capped with SiN_x films. In Fig. 7, the lifetime τ_{eff} (and corresponding J_0) extracted at an injection level of $\Delta n = 2 \times 10^{15}/cm^3$ as a function of cumulative light soaking time, is depicted for p-poly (a, b) and n-poly (c, d). Two degradation cycles were observed for all samples fired between 646 and 744 °C. We recall from the previous sections that the samples with $T_F \geq 792$ °C suffered severe degradation with ruptured blisters on the samples and had comparatively lower lifetimes at the start of the 1-sun stability test.

Two consecutive degradation and recovery cycles, and the onset of a third degradation, were observed. The initial degradation occurred only after 0.08 h in both p-and n-poly samples and was fully recovered after 1 h of exposure. This very fast degradation can be attributed to the well-known boron-oxygen (BO) [37] defect. The relatively flat J_0 values and increasing iV_{OC} (not shown) during this initial lifetime degradation suggest that the BO bulk defect is likely responsible for this initial degradation which is consistent with other findings [38]. Additional IDLS analysis was carried out on the measured lifetimes of the p-poly samples i) after firing and ii) at the point of maximum degradation after 0.08 h. Using a mid-gap energy level, as the exact energy level remains unknown, capture cross-section ratios, k_{LS}, of the defect formed after light soaking for 0.08 h was evaluated for the samples fired at 700, 725, and 744 °C and was found as 19.2, 15.8, 18 respectively. These values are similar to those previously derived for BO degradation [39].

The degradation was more severe in n-poly samples which featured comparatively higher lifetimes than p-type, with some increase in J_0 observed for higher firing temperatures, and the extent of degradation increased with increasing firing temperature. The BO defect was not observed for $T_F < 700$ °C. The maximum subsequent secondary degradation occurred after ~350 h and exhibited less severity in n-poly than the initial BO degradation, where the lifetime at maximum secondary degradation was still higher than the initial values. In p-poly samples, however, the maximum degradation was more severe than the initial BO degradation and even more so with decreasing firing temperature. The p-poly sample fired at 646 °C reached a maximum degradation after ~800 h. We note that the almost imperceptible changes in the sample fired at 646 °C during the first degradation cycle were not due to the lower starting lifetime, as the same sample shows significant lifetime degradation during the second cycle. The evolution of J_0, which increases by up to 100% in p-poly and 70% in n-poly, indicates that the changes are primarily due to degradation in surface passivation. Continual exposure to illumination mostly recovers the n-poly samples, but not the p-poly samples, to post-BO deactivation levels. After light soaking for over 350 days, the onset of a tertiary degradation was seen. In n-poly, the increase in J_0 is more significant than the previous degradations observed but less so in p-poly. The high number of handling steps caused some handling marks to appear (PL images not shown), which invariably would contribute to the loss in passivation exhibited. Nonetheless, as Fig. 7 shows, the unfired samples, which were processed and handled similarly, show remarkable stability throughout the illumination duration in both p- and n-poly samples and highlight the fact that the degradation exhibited is firing-induced and occurs irrespective of poly doping.

Next, we investigate the changes in the samples fired at $T_F \geq 792$ °C after light soaking. As mentioned earlier, these samples exhibited severe blistering, with ruptured blisters and partial delamination of the poly layer observed in some samples (Fig. 3). The decreasing concentration of *N*–H peaks with increasing firing temperature (Fig. 3b) further suggests a greater release of H due to higher thermal energy. Whilst all samples did not show the same level of blistering and delamination, severe degradation of a lifetime was observed for all SiN_x-capped samples fired

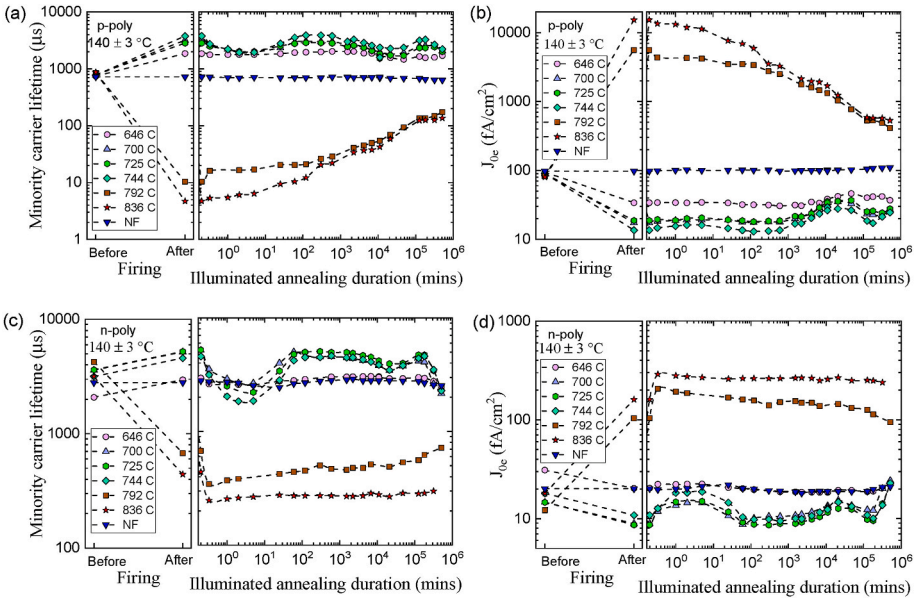

Fig. 7. (a) τ_{eff} (p-poly) and (b) J_{0s} (p-poly), and similarly (c) τ_{eff} (n-poly) and (d) J_{0s} (n-poly) during illuminated annealing at 1-sun and 140 °C. τ_{eff} was extracted at $\Delta n = 2 \times 10^{15}/cm^3$. NF refers to "non-fired" samples.

at this temperature range. The initial 20 s exposure to light, while leading to a rapid deterioration of almost 50% of the already degraded post-fired lifetime in the n-poly samples, enhances the lifetime in p-poly samples. One reason could be that the p-poly already suffered the most severe degradation with lifetimes <10 μs, making further degradation unnoticeable. Further exposure leads to an unexpected and significant improvement in surface passivation in p-poly samples. The 836 °C-fired samples, which had the most severe firing-induced degradation, improved almost 30-fold (similar changes in the 892 °C-fired sample) compared to the post-firing state, with lifetime enhancement from 4.7 μs to 135 μs, a strong reduction in J_0 from >10,000 fA/cm^2 to 534 fA/cm^2 and an iV_{OC} improvement of 84 mV (not shown). In the n-poly samples, no changes were observed for the 836 °C-fired samples, but improvements were seen in the 792 °C-fired samples. The strong recovery observed, considering the blistering and loss of passivation layers on the poly surface, was quite unexpected. Although the recovery did not lead to lifetime values measured prior to firing within the time frame of exposure (365 days), it does not appear to have plateaued and may continue to improve with further illuminated annealing.

Historically, hydrogen has been shown to contribute to BO-LID and LeTID defect reactivation. In BO-LID, hydrogen dissociation from passivated BO complex at high temperatures (in the dark) allows the recombination active defect to reform upon exposure to light [40]. In LeTID, hydrogen released from a bulk hydrogen reservoir triggers a recombination-active complex [41]. In a separate work on n-type Si wafers, the degradation and complete recovery occurred after ~270 h [8]. The degradation and recovery observed in this study, and an onset of a tertiary degradation after over 365 days, raises serious concerns about the long-term stability of passivating contact structures on p-Si wafers and shows similarities with H-related degradation and recovery earlier referenced.

To investigate the potential role of hydrogen in the degradation and recovery observed after firing, we perform some ToF-SIMS measurements to evaluate the depth profile of H in the samples at various stages of the experiment: prior to HT firing, after firing (at 646 °C and 836 °C), after LS (partial recovery). The samples used for ToF-SIMS analysis were obtained from the same batch as previous sections but fired separately. Again, as noted in Fig. 2, firing at 646 °C led to an improved effective lifetime (752 μs–1629 μs), while firing at 836 °C degraded the samples (>700 μs–~4 μs). Light soaking of the degraded sample (for 17 days) led to significant improvement in surface passivation, highlighting the repeatability and agreeing with the results earlier presented (Fig. 5). ToF-SIMS analysis was then carried out on all four samples to observe the distribution of hydrogen up to 400 nm etch depth.

In the ToF-SIMS result shown in Fig. 8, expectedly, a higher H content is observed in the H-rich SiN_x regions. A lower [H] is measured on samples fired at 836 °C for those regions, in agreement with FTIR results earlier presented, showing reduced *N*–H stretching bond density after the high-temperature firing. One significant difference between the 836 °C-fired samples, which showed severe lifetime deterioration, and the other samples (unfired and fired at 646 °C), is the magnitude of hydrogen build-up at the SiO_x interface. The presence of a silicon oxide layer can block H and decrease H flux to underlying layers by orders of magnitude [42]. As such, this is not very surprising and occurs about an order of magnitude higher for samples fired at 836 °C. Further, the concentration of hydrogen in the poly layer and the c-Si is higher in the 836 °C-fired samples. Kang et al. have suggested that such build-up of hydrogen at the interface and excess hydrogenation of the stack is responsible for the deterioration of surface passivation [19]. Our results here agree with that suggestion, as the observed deterioration coincides with the massive build-up of hydrogen at the SiO_x interface and an increased hydrogen concentration in the poly layer and c-Si bulk.

Comparison of the 646 °C- fired sample, which showed significant post-firing improvement in surface passivation (752 μs–1629 μs), and the others, reveals a higher [H] at the SiN_x-polySi interface and a lower [H] around the SiO_x interface. The result is the opposite for the non-

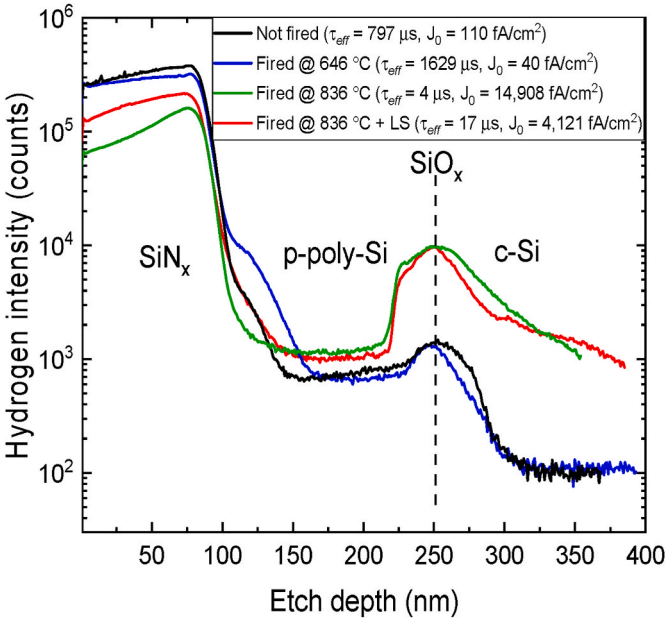

Fig. 8. Hydrogen ToF-SIMS profiles in unfired (black), fired at 646 °C (blue), fired at 836 °C (green) and fired at 836 °C + light-soaked (red) p-type poly samples as a function of etch depth. The fired + LS (light-soaked) sample was analysed (along with other samples) after ~17 days of light soaking. All samples have a SiN_x coating.

light-soaked 836 °C-fired samples (J_0 = 14,908 fA/cm^2). This suggests that while hydrogen does improve surface passivation, an excess amount is undesirable, in agreement with other findings [17,23,43]. Analysis of the light-soaked sample that showed some recovery also points to similar conclusions, with a higher [H] in the poly-Si/SiN_x region than in the non-light-soaked sample but slightly lower in the bulk of the poly and SiO_2/c-Si interface regions.

These ToF-SIMS results aid our understanding of the possible phenomenon underlying the surface passivation recovery after 365 days of light soaking (Fig. 8), but may not be conclusive on their own, as accurately measuring H can be challenging. However, as had been previously suggested, high temperatures may lead to thermal stress at the SiO_x/c-Si interface due to thermal coefficient mismatch [10], and a release of an excess amount of hydrogen from the SiN_x layer. While hydrogen can help passivate some defects, as already observed, it can also lead to other problems. Thus, the density of defects in Si can be multiplied after a firing step. With the excessive hydrogenation at the interface, in-diffusing H can lead to the formation of platelets by incorporating into strained or dangling bonds at the interface, thus, triggering the formation of blisters [31,44,45]. During the long LS that follows, a gradual diffusion of the H through the bulk and the surface could lead to surface passivation improvements.

The diffusivity of H in Si is a key element of hydrogenation and depends on the charge state of hydrogen [46], temperature, excess carrier concentration [47], and concentration of impurities and defects. Fig. 9 by Chen et al. shows a compilation of hydrogen diffusivity data taken from numerous works and converted into the time taken by hydrogen to diffuse through 100 μm of silicon [48]. Accordingly, for a 130 °C LS process, the time for hydrogen to diffuse through a 100 μm wafer could vary between 1×10^5 to 1×10^9 s. The cumulative LS time of 365 days is well within this range, as such, makes hydrogen effusion from the interface and Si bulk a likely explanation for the improvements observed. Since the HT firing process may have induced the generation of a large concentration of defects, it may be that hydrogen effusion will take a longer time in these samples, given the reduced diffusivity known to occur in Si as a result of impurity or defect concentrations [49,50]. If the diffusion of excess hydrogen during LS is responsible for the

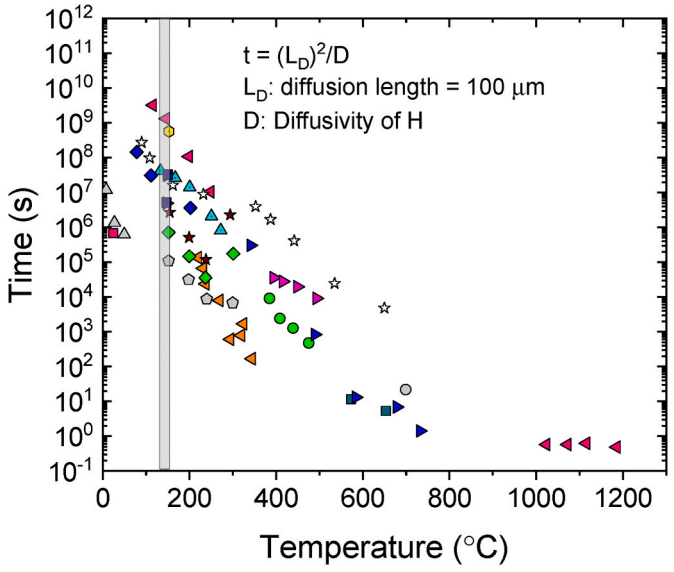

Fig. 9. Hydrogen diffusivity data in mono- and multicrystalline silicon converted into the time required to diffuse through 100 μm, compiled from literature by Chen et al. [48]. The area marked in grey corresponds to the light soaking temperature of 130 °C.

improvement, it is not very clear, however, why the dehydrogenation steps employed, as illustrated in Fig. 6, did not lead to surface passivation improvements. For the blistered samples, it is understandable that the local delamination of the poly Si layers, further deteriorates the surface passivation.

Considering that the degradation and recovery during light soaking are observed only in fired samples, the role of metal complexes formed during the high-temperature process cannot be completely ruled out. In a defect model suggested by Bredemeier et al. metal complexes thought to form following a firing step, can be reconfigured into a recombination-active form during light soaking. Subsequent dissociation yields a highly recombination-active interstitial metal (degradation), which under continued light soaking at elevated temperature, can diffuse to wafer surfaces and crystallographic defects where they become trapped and thus, recombination inactive (recovery). Lesser degradation and a faster recovery in thinner samples have been used to validate this model in high performance mc-Si wafers [51]. The role of metal complexes in the degradation observed in this work, is however left to future work.

The role of the SiN_x-capping layer on the stability of the samples during light soaking was also examined. Fig. 10 shows the changes in τ_{eff}, $J_{0,}$ and iV_{OC} for samples fired and then stripped of SiN_x layer prior to LS for 330 h. Similar conditions were used as presented earlier. For samples fired at $T_F \leq 744$ °C, the results obtained are quite similar for light soaking with nitride layers on. Similar timescales were observed for the first BO-LID degradation and recovery cycle. The onset of the second degradation also occurs in identical timescales to the results presented in

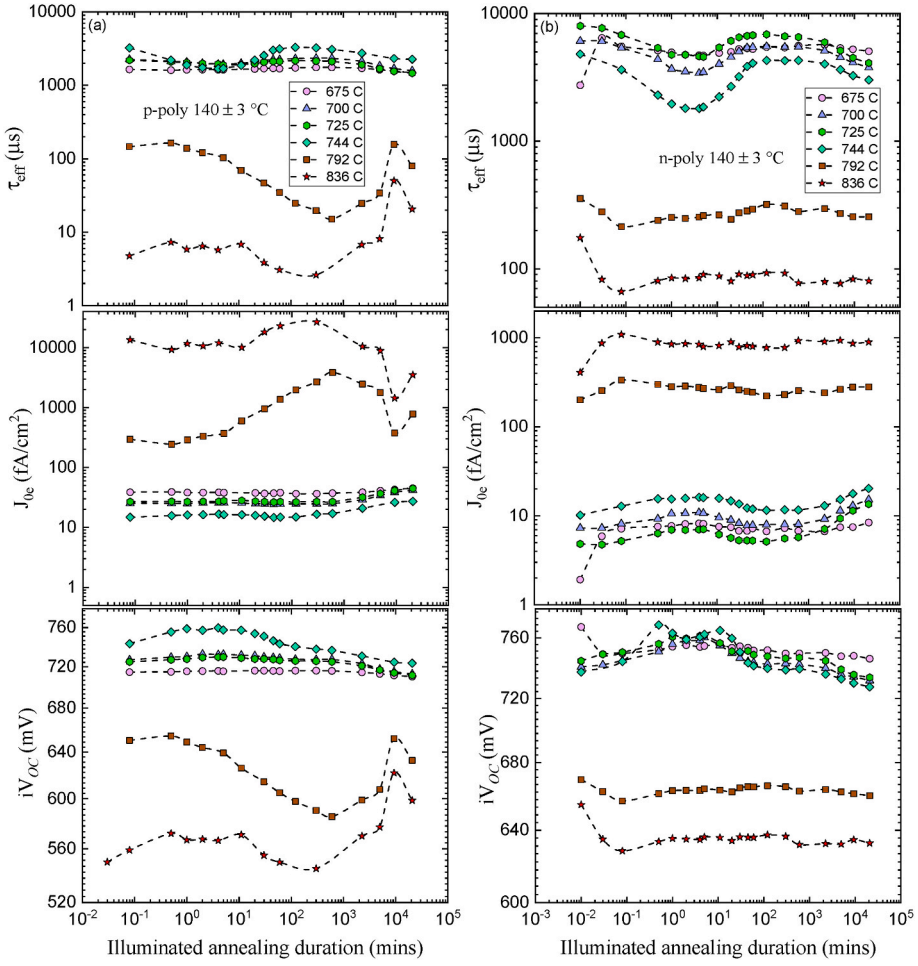

Fig. 10. Light soaking at 1-sun and 140 °C for samples stripped of SiN_x (in HF) after firing, for (a) p-poly: τ_{eff}, J_{0s}, iV_{OC}; and (b) n-poly: τ_{eff}, J_{0s}, iV_{OC}. Note the different scales on the y-axis for n-poly vs p-poly samples. τ_{eff} was extracted at $\Delta n = 2 \times 10^{15}/cm.^3$.

Fig. 7. At higher firing temperatures, ($T_F \geq 792$ °C), the notable difference is for p-poly samples which do not show the immediate recovery observed with a nitride capping layer. Rather, as seen in the $T_F = 792$ °C sample, a surprisingly higher lifetime is observed after firing, and a strong degradation and recovery kicks in which was not observed on samples that had a nitride layer. The observations from Fig. 10 suggest that the nitride layer neither plays a critical role in affecting the kinetics of the observed degradations and recovery during LS nor is it required for recovery. In addition, we can conclude that the hydrogen involved in the kinetics observed during LS does not originate from the SiN_x layer after firing, but from the hydrogen introduced into the bulk and interfaces during firing. Compared to n-type Si, passivating contact structures samples based on p-type Si show remarkable stability during LS. In previous work, we showed that the relative changes in J_0 at the point of maximum degradation during LS for n-type Si with n-poly contacts, compared to J_0 after firing, varied from 166% to 550% [8]. The reader is referred to this work for deeper understanding. In that work, firing was done on the same tool as employed in this work, with similar temperature ranges. The samples, however, were processed differently and on n-type Si wafers, so, direct comparisons may not lead to accurate conclusions. Yet, it is noteworthy that the differences in the magnitude of degradation may suggest that p-type Si may offer better long-term stability compared to n-type. If we consider the n-poly sample fired at 744 °C in this work (which showed the most degradation), at the point of maximum degradation, the J_0 and % increase in J_0 is approximately 19 fA/cm^2 and 73% respectively, while for a similar firing temperature on n-type Si, the values were 62 fA/cm^2 and 480%. The differences are staggering and are worth considering for further investigation in the broader context of increasing market share for n-type-based passivating contact solar cells [1].

4. Conclusion

In this work, we have studied the changes that occur post-firing in SiN_x and AlO_x-capped passivating contact samples having either n- or p-poly layers on p-type c-Si wafers. In SiN_x -capped layers, below a firing temperature of 792 °C, improvements on the surface passivation occur, while above this temperature, severe degradation up to 99%, occurs. In AlO_x samples, firing at all temperatures led to surface degradation. At $T_F > 792$ °C, firing was observed to cause significant blistering and delamination of the poly layer and occurred only in the presence of a nitride capping layer. As such, excess hydrogenation and or trapping of the released hydrogen from the nitride layer during firing, were suggested as leading causes. Subsequent dehydrogenation by annealing in N_2 at 300 °C did not lead to improvements in either SiN_x or AlO_x -capped samples. The dissimilarity in surface passivation changes after firing, as compared to other works in literature, suggests that the base polarity or the chemistry of the SiN_x film plays a role in determining whether passivation improves or degrades after firing.

The results from long-term stability tests carried out under 1-sun illumination at 140 °C, reveal that SiN_x-capped samples are prone to surface and bulk-related instabilities. Specifically, BO-LID defects with capture cross-section ratios in the ranges 15.8–19.2 were observed, along with LeTID-like surface defects which occurred after 160 h. The presence of BO-LID defect on high resistivity samples shows the sensitivity of such structures, which might be minimized by utilizing a Gallium-doped substrates. Although Gallium-doped samples have been shown to suffer from other forms of long-term degradation, similar to those observed in this work [52]. The slow degradation observed for the latter is concerning and requires further studies to provide mitigation strategies. A comparison of the extent of degradation in p-type and n-type c-Si, highlights that p-type substrate may provide much better stability. When compared to the literature, the extent of degradation in n-type-based poly-Si samples were observed in some cases to be more than seven (7) times that in p-type and may be related to the variations in hydrogen diffusivity across both doping polarities. Such differences warrant further studies with more direct comparisons on the role of base doping for polysilicon passivating contact samples. Light soaking led to significant surface passivation improvement on blistered samples which were severely degraded after firing. Further analysis of similar samples showed that the recovery may be due to changes in the hydrogen concentration at the SiN_x/polySi and around the SiO_x interfaces, and further highlights the likely involvement of hydrogen in the long-term stability of these structures. Further, we show that the degradation and recovery kinetics observed during light soaking has a temperature dependence but are independent of a nitride capping layer.

CRediT authorship contribution statement

Chukwuka Madumelu: Writing – original draft, Methodology, Investigation, Formal analysis, Data curation, Conceptualization. **Yalun Cai:** Writing – original draft, Investigation, Formal analysis. **Christina Hollemann:** Writing – review & editing, Investigation, Conceptualization. **Robby Peibst:** Supervision, Resources, Funding acquisition. **Bram Hoex:** Writing – review & editing, Supervision. **Brett J. Hallam:** Writing – review & editing, Resources, Project administration, Funding acquisition. **Anastasia H. Soeriyadi:** Conceptualization, Methodology, Supervision.

Declaration of competing interest

The authors declare that they have no known competing financial interests or personal relationships that could have appeared to influence the work reported in this paper.

Data availability

Data will be made available on request.

Acknowledgments

This work was supported by the Australian Government through the Australian Renewable Energy Agency (ARENA: 2017/RND003). AS acknowledges the support by the Australian Government through the Australian Renewable Energy Agency (ARENA) and the Australian Centre for Advanced Photovoltaics (ACAP). The views expressed herein are not necessarily the views of the Australian Government, and the Australian Government does not accept responsibility for any information or advice contained herein. This work was supported by the British Council under PAK-UK ICRG 2020 grant number 006327/D/ISB/008/2021. The authors would also like to acknowledge the Solar Industrial Research Facility (SIRF) and the Surface Analysis Laboratory, SSEAU, MWAC, UNSW for the provision of facilities and equipment used for characterization. CH thankfully acknowledges the German Federal Ministry for Economic Affairs and Climate Action and the state of Lower Saxony for funding this work.

References

[1] International Technology Roadmap for Photovoltaic (ITRPV), itrpv.vdma.org; 13th edition, 2022. pp. .1-81.
[2] R. Peibst, M. Rienäcker, Y. Larionova, et al., Towards 28%-efficient Si single-junction solar cells with better passivating POLO junctions and photonic crystals, Sol. Energy Mater. Sol. Cells 238 (2022), 111560.
[3] S. Mack, J. Schube, T. Fellmeth, F. Feldmann, M. Lenes, J. Luchies, Metallisation of boron-doped polysilicon layers by screen printed silver pastes, Phys. Status Solidi Rapid Res. Lett. 11 (12) (2017), 1700334.
[4] F. Haase, C. Hollemann, S. Schäfer, et al., Laser contact openings for local poly-Si-metal contacts enabling 26.1%-efficient POLO-IBC solar cells, Sol. Energy Mater. Sol. Cells 186 (2018) 184–193, https://doi.org/10.1016/j.solmat.2018.06.020.
[5] A. Richter, R. Müller, J. Benick, et al., Design rules for high-efficiency both-sides-contacted silicon solar cells with balanced charge carrier transport and recombination losses, Nat. Energy 6 (4) (2021) 429–438, https://doi.org/10.1038/s41560-021-00805-w, 2021 64.
[6] M. Winter, S. Bordihn, R. Peibst, R. Brendel, J. Schmidt, Degradation and regeneration of n+-doped poly-Si surface passivation on p-type and n-type cz-Si

under illumination and dark annealing, IEEE J. Photovoltaics 10 (2) (2020) 1–8, https://doi.org/10.1109/jphotov.2020.2964987.
[7] D. Kang, H.C. Sio, D. Yan, et al., Long-term stability study of the passivation quality of polysilicon-based passivation layers for silicon solar cells, Sol. Energy Mater. Sol. Cells 215 (June) (2020), 110691, https://doi.org/10.1016/j.solmat.2020.110691.
[8] D. Chen, C. Madumelu, M. Kim, et al., Investigating the degradation behaviours of n+-doped Poly-Si passivation layers: an outlook on long-term stability and accelerated recovery, Sol. Energy Mater. Sol. Cells 236 (May 2021) (2022), 111491, https://doi.org/10.1016/j.solmat.2021.111491.
[9] C. Hollemann, F. Haase, S. Schäfer, J. Krügener, R. Brendel, R. Peibst, 26.1%-efficient POLO-IBC cells: quantification of electrical and optical loss mechanisms, Prog. Photovoltaics Res. Appl. 27 (11) (2019) 950–958, https://doi.org/10.1002/PIP.3098.
[10] C. Hollemann, M. Rienäcker, A. Soeriyadi, et al., Firing stability of tube furnace-annealed n-type poly-Si on oxide junctions, Prog. Photovoltaics Res. Appl. (2021), https://doi.org/10.1002/PIP.3459.
[11] A.H. Soeriyadi, C. Hollemann, C. Madumelu, et al., Impact of firing and capping layers on long-term stability of doped poly-Si passivating contact layers, AIP Conf. Proc. 2487 (2022), 50006. AIP Publishing LLC.
[12] B.J. Hallam, C.E. Chan, R. Chen, et al., Rapid mitigation of carrier-induced degradation in commercial silicon solar cells, Jpn. J. Appl. Phys. 56 (8) (2017), https://doi.org/10.7567/JJAP.56.08MB13, 0-6.
[13] B.J. Hallam, P.G. Hamer, A.M. Ciesla née Wenham, C.E. Chan, B. Vicari Stefani, S. Wenham, Development of advanced hydrogenation processes for silicon solar cells via an improved understanding of the behaviour of hydrogen in silicon, Prog. Photovoltaics Res. Appl. 28 (12) (2020) 1217–1238, https://doi.org/10.1002/pip.3240.
[14] B. Wright, C. Madumelu, A. Soeriyadi, M. Wright, B. Hallam, Evidence for a light-induced degradation mechanism at elevated temperatures in commercial N-type silicon heterojunction solar cells, Sol RRL 2000214 (2020) 1–5, https://doi.org/10.1002/solr.202000214.
[15] C. Madumelu, B. Wright, A. Soeriyadi, et al., Investigation of light-induced degradation in N-Type silicon heterojunction solar cells during illuminated annealing at elevated temperatures, Sol. Energy Mater. Sol. Cells 218 (2020), 110752, https://doi.org/10.1016/j.solmat.2020.110752.
[16] D. Kang, H.C. Sio, J. Stuckelberger, et al., Optimum hydrogen injection in phosphorus-doped polysilicon passivating contacts, ACS Appl. Mater. Interfaces (2021), https://doi.org/10.1021/acsami.1c17342.
[17] C. Hollemann, M. Rienäcker, A. Soeriyadi, et al., Firing stability of tube furnace-annealed n-type poly-Si on oxide junctions, Prog. Photovoltaics Res. Appl. 30 (1) (2022) 49–64, https://doi.org/10.1002/pip.3459.
[18] D. Kane, S. Richard, Measurement of the emitter saturation current by a contactless photoconductivity decay method, in: IEEE Photovoltaic Specialists Conference, 1985, pp. 578–583.
[19] D. Kang, H.C. Sio, J. Stuckelberger, et al., Comparison of firing stability between p- and n-type polysilicon passivating contacts, Prog. Photovoltaics Res. Appl. (2022), https://doi.org/10.1002/PIP.3544.
[20] Choi S, Kwon O, Hong Min K, et al. Formation and Suppression of Hydrogen Blisters in Tunnelling Oxide Passivating Contact for Crystalline Silicon Solar Cells. doi:10.1038/s41598-020-66801-4.
[21] Nemeth B, Young DL, Page MR, et al. INVITED FEATURE PAPER Polycrystalline Silicon Passivated Tunneling Contacts for High Efficiency Silicon Solar Cells. doi: 10.1557/jmr.2016.77.
[22] M. Fırat, H.S. Radhakrishnan, S. Singh, et al., Industrial Metallization of Fired Passivating Contacts for N-type Tunnel Oxide Passivated Contact (N-TOPCon) Solar Cells, 2022, https://doi.org/10.1016/j.solmat.2022.111692.
[23] D. Kang, H.C. Sio, J. Stuckelberger, et al., Optimum hydrogen injection in phosphorus-doped polysilicon passivating contacts, ACS Appl. Mater. Interfaces 13 (46) (2021) 55164–55171, https://doi.org/10.1021/ACSAMI.1C17342.
[24] Z. Peng, S. Chen, Peeling behavior of a thin-film on a corrugated surface, Int. J. Solid Struct. 60 (2015) 60–65, https://doi.org/10.1016/J.IJSOLSTR.2015.02.003.
[25] H.E. Çiftpinar, M.K. Stodolny, Y. Wu, et al., Study of screen printed metallization for polysilicon based passivating contacts, Energy Proc. 124 (2017) 851–861, https://doi.org/10.1016/J.EGYPRO.2017.09.242.
[26] A. Cuevas, T. Allen, J. Bullock, Y. Wan, D. Yan, X. Zhang, Skin care for healthy silicon solar cells, IEEE 42nd Photovolt Spec Conf PVSC (2015), https://doi.org/10.1109/PVSC.2015.7356379, 2015. 2015;(1.
[27] R.S. Bonilla, B. Hoex, P. Hamer, P.R. Wilshaw, Dielectric Surface Passivation for Silicon Solar Cells: A Review, 2017, https://doi.org/10.1002/pssa.201700293.
[28] Y. Yang, P.P. Altermatt, Y. Cui, et al., Effect of carrier-induced hydrogenation on the passivation of the poly-Si/SiO x/c-Si interface, AIP Conf. Proc. (2018), https://doi.org/10.1063/1.5049289, 1999(August.
[29] D. Yan, S.P. Phang, Y. Wan, C. Samundsett, D. Macdonald, A. Cuevas, High efficiency n-type silicon solar cells with passivating contacts based on PECVD silicon films doped by phosphorus diffusion, Sol. Energy Mater. Sol. Cells 193 (2019) 80–84, https://doi.org/10.1016/J.SOLMAT.2019.01.005.
[30] M. Vaqueiro-Contreras, V.P. Markevich, M.P. Halsall, et al., Powerful recombination centers resulting from reactions of hydrogen with carbon–oxygen defects in n-type Czochralski-grown silicon, Phys. Status Solidi Rapid Res. Lett. 11 (8) (2017), 1700133, https://doi.org/10.1002/PSSR.201700133.
[31] N.H. Nickel, G.B. Anderson, N.M. Johnson, J. Walker, Nucleation of Hydrogen-Induced Platelets in Silicon, 62, 2000.
[32] M.A. Roberson, S.K. Estreicher, Vacancy and vacancy-hydrogen complexes in silicon, Phys. Rev. B 49 (24) (1994).
[33] A.C.N. Wenham, S. Wenham, R. Chen, et al., Hydrogen-Induced Degradation, IEEE 7th World Conf Photovolt Energy Conversion, WCPEC 2018 - A Jt Conf 45th IEEE PVSC, 28th PVSEC 34th EU PVSEC, 2018, pp. 1–8, https://doi.org/10.1109/PVSC.2018.8548100, 2018.
[34] D. Chen, P.G. Hamer, M. Kim, et al., Hydrogen induced degradation: a possible mechanism for light- and elevated temperature- induced degradation in n-type silicon, Sol. Energy Mater. Sol. Cells 185 (April) (2018) 174–182, https://doi.org/10.1016/j.solmat.2018.05.034.
[35] B.W.H. van de Loo, B. Macco, M. Schnabel, et al., On the hydrogenation of Poly-Si passivating contacts by Al2O3 and SiNx thin films, Sol. Energy Mater. Sol. Cells (2020) 215, https://doi.org/10.1016/J.SOLMAT.2020.110592.
[36] G. Dingemans, A.P. Wb, undefined. Hydrogen induced passivation of Si interfaces by films and stacks, aip.scitation.org (2010). https://aip.scitation.org/doi/abs/10.1063/1.3497014?casa_token=eVOgnaBMBMQAAAAA:rIbJ81nB3b-vknLAvn0i5I1TY_Mz7jh8Yo2sBQLblW7FeMuBSbH_9ZZRicGgkfgHzKO-ezuVE4w. (Accessed 2 April 2022).
[37] J. Schmidt, Light-induced Degradation in Crystalline Silicon Solar Cells, 2004. www.scientific.net/SSP.95-96.187.
[38] M. Winter, S. Bordihn, R. Peibst, R. Brendel, J. Schmidt, Degradation and regeneration of n+-doped poly-Si surface passivation on p-type and n-type cz-Si under illumination and dark annealing, IEEE J. Photovoltaics 10 (2) (2020) 423–430, https://doi.org/10.1109/jphotov.2020.2964987.
[39] D. Chen, Elucidating the Mechanics behind Light- and Elevated Temperature-Induced Degradation in Silicon Solar Cells, 2020;(February.
[40] J. Schmidt, A.G. Aberle, R. Hezel, Investigation of carrier lifetime instabilities in Cz-grown silicon, Conf. Rec. IEEE Photovolt. Spec. Conf. (1997) 13–18.
[41] T.H. Fung, M. Kim, D. Chen, et al., A four-state kinetic model for the carrier-induced degradation in multicrystalline silicon: introducing the reservoir state, Sol. Energy Mater. Sol. Cells 184 (2018) 48–56, https://doi.org/10.1016/J.SOLMAT.2018.04.024.
[42] N.H. Nickel, W.B. Jackson, I.W. Wu, C.C. Tsai, A. Chiang, Hydrogen permeation through thin silicon oxide films, Phys. Rev. B 52 (11) (1995) 7791.
[43] C. Hollemann, N. Folchert, S.P. Harvey, et al., Changes in hydrogen concentration and defect state density at the poly-Si/SiOx/c-Si interface due to firing, Sol. Energy Mater. Sol. Cells 231 (2021), 111297, https://doi.org/10.1016/J.SOLMAT.2021.111297.
[44] N.H. Nickel, G.B. Anderson, J. Walker, Hydrogen-induced platelets in disordered silicon, Solid State Commun. 99 (6) (1996) 427–431, https://doi.org/10.1016/0038-1098(96)00283-9.
[45] N.M. Johnson, F.A. Ponce, R.A. Street, R.J. Nemanich, Defects in c-Si induced by hydrogenation, Phys. Rev. B 35 (8) (1987) 4166–4169.
[46] D. Mathiot, Modeling of hydrogen diffusion in n- and p-type silicon, Phys. Rev. B 40 (8) (1989) 5867–5870, https://doi.org/10.1103/PhysRevB.40.5867.
[47] C. Sun, F.E. Rougieux, D. Macdonald, A unified approach to modelling the charge state of monatomic hydrogen and other defects in crystalline silicon, J. Appl. Phys. 117 (4) (2015), https://doi.org/10.1063/1.4906465.
[48] D. Chen, M. Kim, J. Shi, et al., Defect engineering of p-type silicon heterojunction solar cells fabricated using commercial-grade low-lifetime silicon wafers, Prog. Photovoltaics Res. Appl. 29 (11) (2021) 1165–1179, https://doi.org/10.1002/pip.3230.
[49] C.P. Herrero, M. Stutzmann, A. Breitschwerdt, P.V. Santos, Trap-limited hydrogen diffusion in doped silicon, Phys. Rev. B 41 (2) (1990) 1054, https://doi.org/10.1103/PhysRevB.41.1054.
[50] T. Zundel, J. Weber, Trap-limited hydrogen diffusion in boron-doped silicon, Phys. Rev. B 46 (4) (1992) 2071, https://doi.org/10.1103/PhysRevB.46.2071.
[51] D. Bredemeier, D. Walter, J.S.-S. Rrl, undefined. Possible candidates for impurities in mc-Si wafers responsible for light-induced lifetime degradation and regeneration, Wiley Online Libr 2 (1) (2018), https://doi.org/10.1002/solr.201700159, 2017.
[52] D. Lin, Z. Hu, L. Song, D. Yang, X. Yu, Investigation on the light and elevated temperature induced degradation of gallium-doped Cz-Si, Sol. Energy 225 (2021) 407–411.
[53] D. Kang, H.C. Sio, J. Stuckelberger, et al., Comparison of firing stability between p- and n-type polysilicon passivating contacts, Prog. Photovoltaics Res. Appl. (2022; (February), https://doi.org/10.1002/pip.3544.
[54] D. Kang, H.C. Sio, J. Stuckelberger, et al., Firing Stability of Polysilicon Passivating Contacts: the Role of Hydrogen, August 2021, https://doi.org/10.1109/PVSC43889.2021.9519080, 0701-0705.
[55] A. Morisset, R. Cabal, B. Grange, et al., Highly passivating and blister-free hole selective poly-silicon based contact for large area crystalline silicon solar cells, Sol. Energy Mater. Sol. Cells 200 (2019), 109912.